Forecasting Pest Risk Level in Roses Greenhouse: Adaptive Neuro-Fuzzy Inference System vs Artificial Neural Networks

Ahmad Tay, Frédéric Lafont, Jean-François Balmat

Forecasting Pest Risk Level in Roses Greenhouse: Adaptive Neuro-Fuzzy Inference System vs Artificial Neural Networks

Ahmad Tay*, Frédéric Lafont, Jean-François Balmat

University of Toulon, LIS, UMR CNRS 7020, Bt X,CS 60584, 83041 Toulon cedex 9, France

Abstract

The purpose of this study is to establish a system for the prediction of the pests' risk level in a roses greenhouse by applying Artificial Neural Networks (ANNs) and an Adaptive Neuro-Fuzzy Inference System (ANFIS). Pests in roses greenhouses are known to be fatal to plants if not detected at a premature stage. Early detection could avoid huge agronomic and economic losses. Though, it could be a difficult task to achieve. The complexities arising from the interactions between variables influencing the development could be a barrier to fulfill the previously mentioned task. The output of the developed system represents the next day's risk level of Western flower Thrips (WFT) (*Frankliniella occidentalis*) in a roses greenhouse. Four explanatory variables, such as internal temperature, internal humidity, today's pest risk level and human intervention have been considered for this estimation. The main contributions of this study are three fold; providing a daily estimate WFT risk level, reducing the use of pesticides and finally mitigating yield loss. The obtained results were compared to each other and to real data. The performance of the models has been evaluated by 3 statistical indicators. Numerical results showed conspicuous performance of both models, indicating their efficiency for pest monitoring. The novelty associated with the system is the creation of decision support tool for daily risk assessment of WFT. Relying on a small number of variables, this system is a monitoring tool which contributes to help farmers early reveal warning signs. In addition, this is a first attempt to employ ANNs and ANFIS for the prediction of WFT.

Keywords: Decision Making, Artificial Neural Networks, ANFIS, Risk Assessment, Integrated Pest Management

*Corresponding author
Email address: ahmad.tay@univ-tln.fr (Ahmad Tay)

1. Introduction

Western Flower Thrips (WFT), or *Frankliniella occidentalis* (Pergande 1895), is a polyphagous pest species in horticulture and agriculture worldwide. The origin of this species of thrips is the North-West of America and Mexico [1]. The presence of *F. occidentalis* was reported for the first time in Europe in 1983 and in 1986 on French territory, and since then it is considered a cosmopolitan serious pest [2]. This pest insect attack ornamental crops, trees and vegetables, and lead to enormous economical and agricultural losses. Their tiny size, high and fast reproduction rate, affinity for protected zones and their behavior on host plants (difficulty to predict the way they shift from leaves into rosebuds) hinder their early detection [3]. Accordingly, and in addition to the fact that *F. occidentalis* feed on flowers, leaves and on other herbivores [3], they cause a vast economic damage. It is then essential to adopt Integrated Pest Management (IPM) programs. IPM involves the implementation of several control protocols such as chemical (pesticides), biological, physical and others ([4] and therein). Separate carrying out of those approaches had not led to auspicious consequences. For example, the huge dependence on pesticides led to the resistance of pests to them, and hindered their efficiency. It is hence more preferable to adopt other practices or combine several strategies for a better control of WFT [5, 6]. Among the eight IPM principles [6], monitoring (aka scouting [7, 8]) is one of the most important tactics to control WFT. Scouting is defined as counting and estimating population densities of a pest species [9]. It helps detect harmful organisms and it incorporates two methods [10]: direct sampling by tapping flower heads, and indirect sampling using yellow sticky traps. Thrips population densities could be also estimated using computational and mathematical models and early diagnosis systems with the help of professional advisors [6].

Many models have been developed to estimate thrips population. The joint purpose of these models is to serve as a potential decision tool. Ogada et al. [11] introduced a deterministic model consisting of differential equation systems to estimate thrips population growth by incorporating the effect of Tomato Spotted Wilt Virus (TSWV) on its dynamic. The model required a huge number of variables to be constructed (18 variables). A mathematical model was built to estimate WFT on greenhouse grown chrysanthemum by considering the temperature, population density and food availability [12]. Wang [13] predicted population dynamics of *F. occidentalis* depending on females' fecundity, sex ratio and larval mortality. Many other approaches have been developed for modeling insects populations ([10, 14, 15] and therein). None of the models was established to provide a

real-time daily estimate. They also required too many variables which are difficult to obtain by regular farmers (sticky traps, amount of eggs in infected plants, sex, leaves damages, etc.). Certain models were established under laboratory conditions, unconcerned with complexities arising from interactions inside the greenhouse [14, 16]. These difficulties drive us to avail Soft Computing (SC) to design an eligible model to estimate *F. occidentalis* population in a roses greenhouse.

Soft Computing is the establishment of approximate models to solve real complex problems which include uncertainty, and impreciseness. Artificial Neural Networks (ANNs) and Adaptive Network-based Fuzzy Inference System (ANFIS) are critical algorithms for SC [17]. ANNs are nonlinear algebraic computational models introduced by McCulloch and Pitts in 1943 [18], based on the biological neural network. ANFIS is a fuzzy system developed by exploiting the similarities between Fuzzy Logic (FL) and certain forms of neural networks. ANFIS was first proposed by J.-S. Jang for system identification and time series prediction [19].

Artificial Neural Networks have been a major subject for applications in many fields including agriculture. They have shown robust performances when it comes to prediction of disease and pests. ANNs were applied to estimate weekly population of thrips per leaf in cotton crops [20], monthly populations of Melon thrips and Diamondback moth [21], incidence of rust in coffee [22], monthly wheat Deoxynivalenol [23], and the geographic distribution of pests [24]. They were also employed to estimate other crop diseases and pests ([25, 26, 27]). As for ANFIS, it has been used in agriculture due to its ability to structure nonlinear relation between a set of predictors and a set of dependent variables. It was employed for the classification of different types of diseases of tomato and brinjal/eggplant via features extraction [28]. ANFIS was also utilized to classify three cotton leaf's diseases [29] and for the diagnosis of soya-beans diseases [30], but not yet for WFT risk estimation in roses production.

Our study aims to assist farmers and decision makers to monitor the population of WFT in roses greenhouses by introducing ANNs and ANFIS models. One of the main advantages of this study is that the model provides a daily risk index, unlike other models which give weekly estimates. This advantage is very substantial for IPM because it could help farmers to employ appropriate strategies based on the displayed signal. Also, we are interested in developing a model to predict thrips populations in a roses greenhouse, relying on a small number of variables. Selecting

few descriptors, meaning the dependence on few sensors, is an important aspect because some greenhouses might not be equipped with many sensors, due to their expensive prices, and difficulty to use and understand.

The incentives of this work are to avoid yield loss, to optimize the production by reducing the use of pesticides, and to help the farmer effectively against WFT. The aspects of this study are interesting just as the system discloses a daily risk value, notifying the user about the risk level in the greenhouse. As this project is a collaboration between the university of Toulon and the Technical Institute of Horticulture (ASTREDHOR), the obtained results were validated by experts with whom we collaborate, at the Syndicate of the Regional Center for Application and Horticultural Demonstration (SCRADH), its station in Hyères, France.

The rest of paper is organized as follows. Section 2 is dedicated to present the materials and methods in which we introduce the place of the study, the data and the proposed models. Section 3 includes the experimental results. Section 4 presents a discussion about the findings of this research. At the end, a general conclusion is presented. The comparison with FL was not included in this study because we are rather interested in data-based systems than knowledge based.

2. Materials and Methods

2.1. Experimentation's site description

Hyères is a major city in the south-eastern France, known for its importance in producing roses in the French Riviera. The SCRADH, latitude 43° 6' 55.9836" N, longitude 6° 9' 11.663" E, is a center that conducts experiments and research programs in the horticultural sector in Hyères. They have been carrying out experimental protocols on greenhouse crop production systems, then validating the technical and economic feasibility of new production concepts. Their inquiries and explorations are concerned with adopting appropriate strategies to control WFT, which has been an annoying pest since many years. A high percentage of crop loss has been observed (100% at some periods) due to WFT. The experimental greenhouse (300 m^2) consists of 6 benches (B1 to B6) of 24m long each, each carrying 6 plots (Fig. 1) (36 plots in total). Each plot (parcel) measures 4m $\times$1m = 4m^2 and contains about 34 rose-plants of same variety, for instance, Milva 2A, Samourai, Amaretto, Penny

Lane, etc. The plants size varies between [0.5m, 2m] and the average size of the plants is about 1.5m (Fig. 2). None of the plants was withered and replaced during data acquisition period.

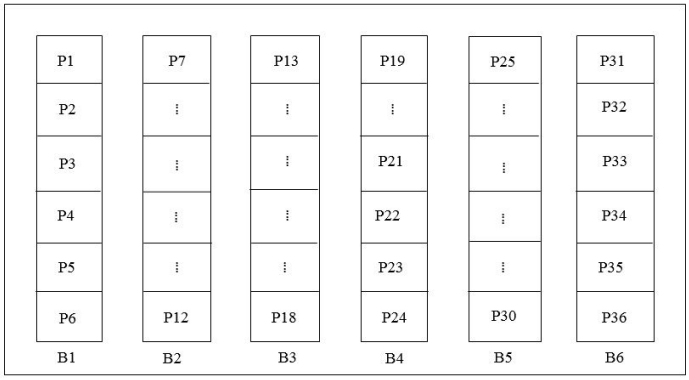

Figure 1: Distribution of plots in the greenhouse [31]

Figure 2: Rose plants at commercial stage and experimentation materials used to tap the rosebuds

2.2. Factors promoting the development of WFT

Temperature and humidity are considered the most important factors affecting WFT development. Olatinwo and Hoogenboom [32] stated all the climatic factors temperature, rainfall, and relative humidity that influence the development of WFT. The effect of relative humidity on the determination of WFT has been discussed by Fatnassi et al. [33] and Steiner et al. [34]. The results of the previously cited studies showed that the perfect temperature for thrips survival is between $23°C$ and $28°C$, while the optimal relative humidity varies between 70% and 80%.
According to SCRADH's expertise and existing literature, the development of WFT is also contingent upon the existing population of WFT, and physical interventions carried out by farmers. The present density of WFT in the greenhouse following survival is important to measure the risk on rose plants. The selection of human intervention is suggested by our partners at SCRADH as a consequence of its effect on reducing thrips density.

2.3. Data acquisition

Data provided by the SCRADH consists of temperature and humidity data measured by sensors and pest data measured by manual counting.

2.3.1. Temperature and humidity data

The hourly internal temperature Ti ($°C$), and internal relative humidity HR (%) data are utilized, and they were recorded between October 2012 and May 2014.

2.3.2. Insect population data

For each plot, 4-5 plants were randomly selected, with 1.5 meters in between. Engineers at SCRADH counted the number of WFT individuals inside the rosebuds (of the selected plants) at harvesting (commercial) stage by threshing each rosebud on a white paper (Fig. 3). The number of WFT in each flower plot tr_i is classified into 4 classes: 0, 1, 2, and 3, respectively corresponding to the total absence, existence of 1, 2, and 3 and more WFT individuals.

Let n_i be the frequency (number of repetitions) of each class tr_i. Since $tr_3 = 3$ corresponds to the existence of 3 and more thrips, then its frequency is considered more significant than the others. For example, even if the counted population is 1000, it is marked 3. When we compute

Figure 3: WFT individuals threshed on white papers

the mean, there will be a loss of information, and the relevant value is not a good representative. For a realistic and logical demonstration, each n_i is associated with a certain weight w_i, such that $w_0 = w_1 = w_2 = 0.1$ and $w_3 = 0.7 = 1 - (w_0 + w_1 + w_2)$. The weights were proposed by the SCRADH's engineers following their expertise, but they could be adjusted depending on strong knowledge in the field. The measured risk level of WFT ($\overline{WFT}_{week}$) in the greenhouse $\in [0, 3]$ is attained as shown below (Eq. (1)):

$$\overline{WFT}_{week} = \frac{\sum_{i=0}^{3} w_i n_i tr_i}{\sum_{i=0}^{3} w_i n_i} \tag{1}$$

As an example, on week 19 in 2013, 0 thrips individuals was detected in 20 plots, only 1 thrips in 8 plots, 2 individuals in 3 plots, and 3 and more in 5 plots (Table 1). We remind that $tr_3 = 3$ corresponds to the presence of 3 and more thrips, and that its frequency $n_3 = 5$ is way more important than others classes.

Table 1: Counting of WFT individuals on week 19 of the year 2013

tr_i	0	1	2	3	total
n_i	20	8	3	5	36
w_i	0.1	0.1	0.1	0.7	1

Accordingly, the measured level of WFT on week 19 of the year 2013 is:

$$\overline{WFT}_{week19} = \frac{0.1 \times 20 \times 0 + 0.1 \times 8 \times 1 + 0.1 \times 3 \times 2 + 0.7 \times 5 \times 3}{0.1 \times 20 + 0.1 \times 8 + 0.1 \times 3 + 0.7 \times 5} = 1.8 \tag{2}$$

Fig. 4 presents the risk values of WFT on all the other weeks of the study, calculated following the same method as the one shown above (Eq. (1)). Each value is defined and interpreted as the risk level of WFT and not the mean value. We are currently working on a method to transform this value into an approximated value of WFT individuals.

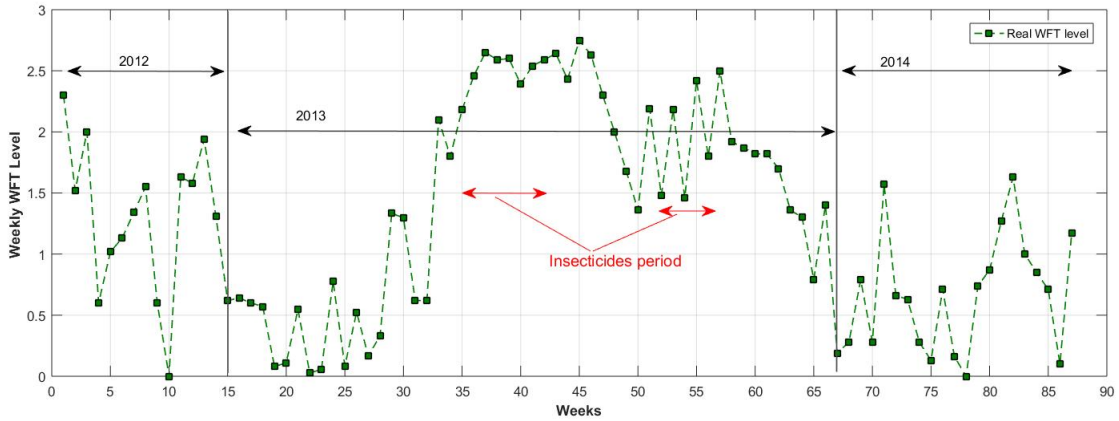

Figure 4: WFT weekly risk levels calculated from Eq. (1)

Since we strive at obtaining a daily prediction of WFT risk level, we calculated the daily averages of $\overline{Ti}$ and $\overline{HR}$ respectively. As for pest data, $\overline{WFT}_{week}$ underwent linear interpolation using newton's formula [35] to approximate the daily WFT risk level ($\overline{WFT}$).

2.3.3. Human intervention

Engineers at SCRADH observed remarkable decreases in WFT populations during human intervention, i.e, Dishooting (DS) (the rosebuds are broken so the plants accumulate nutrients), pruning (PR), and massive harvesting (MH). The population of WFT is respectively reduced by 50% and 90% at the end of PR and MH periods. DS is a weekly performed intervention and leads to the removal of equal WFT subpopulations. Hence, the weekly eliminated percentage is $\frac{100\%}{s}$ where $s \geq 1$ is the number of weeks predetermined for DS. Management practices were performed as follows:

- Dishooting: weeks 46-50.
- Massive harvesting: Christmas holidays (weeks 13-15, 66-67) and Valentine's day (weeks 21-22, 73-74).
- Pruning: weeks 2-3 and 71-72.
- Insecticides: Applied 3 times per month from May to July (weeks 35-42) and between September and October (weeks 52-56) (Fig. 4).

By reason of the fact that a significant shortage of knowledge about the removed daily quantities exists, we consider that equal subgroups are withdrawn. For a clear demonstration, the daily eliminated percentage due to PR, MH, and DS are correspondingly $\frac{50\%}{D1}$, $\frac{90\%}{D2}$, and $\frac{100\%}{7s}$. The daily weighting coefficients $\gamma(t)$ of each of the intervention phases can be written as follows:

$$\gamma(t) = \begin{cases} (1 - 0.5/D1) & PR = 1 \\ (1 - 0.9/D2) & MH = 1 \\ (1 - \frac{1}{7s}) & DS = 1 \\ 1 & otherwise \end{cases} \tag{3}$$

where D1 and D2 are the planned durations of PR and MH in days respectively. For instance, if we plan to prune the plants over 6 days (D1=6 days), then the daily weighting coefficient is $\gamma(t) = 1 - 0.08 = 0.92$. Considering one week of DS, i.e, s=1, then $\gamma(t) = 1 - 1/7 = 0.85$.

2.4. Artificial neural networks ANNs

ANNs can be defined as mathematical models or data-processing systems that simulate biological neurons. ANNs are considered as function approximations to model complex and nonlinear relationships between a set of outputs and a set of inputs [20]. The Feed Forward neural network (FFNN) or multilayer perceptron (Fig. 5) is one of the mostly used and efficient network among other ANN prototypes [36]. The output of the k^{th} node of the hidden layer can be written as:

$$H_k = f(\sum_{j=1}^{P} w_{k,j} X_j + b_1^k) \tag{4}$$

where w_{kj} are the weights connecting the j^{th} input and the k^{th} hidden neuron, and b_1^k is the bias of the k^{th} neuron. The activation function f could be sigmoid, linear, tangent hyperbolic or any other defined differentiable function. The output of the network is the estimated target variable, and its calculation depends on the outputs of previous hidden layer and other connection weights between the outputs nodes and the hidden nodes. It is mathematically expressed as follows:

$$O_l = g(\sum_{l=1}^{L} w_{l,k}^{\star} H_k + b_2^l) \tag{5}$$

where $w_{lk}^{\star}$ are the weights connecting the k^{th} hidden neuron with the l^{th} output neuron, and b_l^2 is the bias of the l^{th} output neuron. The value of the activation function g is the predicted output of the network O_l. As they are data driven models, ANNs use learning algorithms [37] to adjust

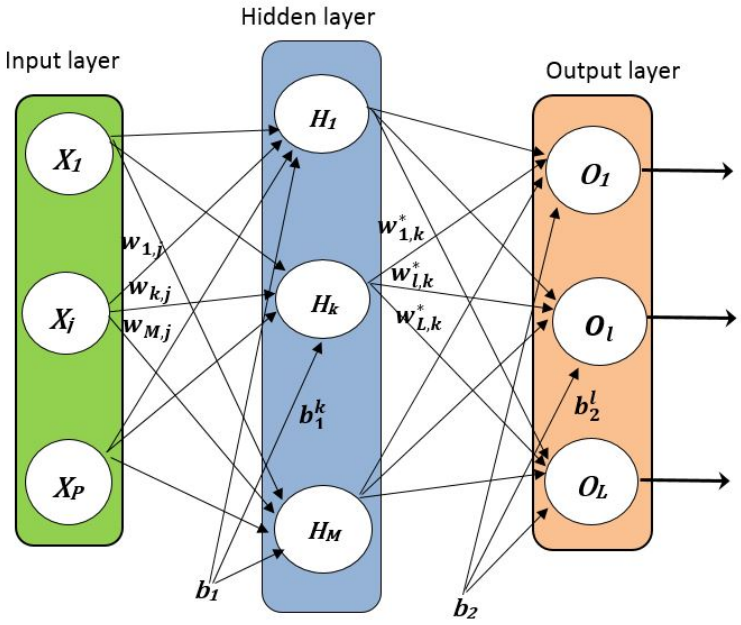

Figure 5: Typical architecture of an FFNN with one hidden layer

the connections of the network in order to obtain the best operating model. This model is obtained when the error E_{total} is minimized to a certain threshold:

$$E_{total} = \frac{1}{N}\sum_{i=1}^{N}(\frac{1}{2}\sum_{l=1}^{L}(O_l - Y_l)^2) \tag{6}$$

where N is the total number of training samples, L is the number of outputs, $(\frac{1}{2}\sum_{l=1}^{L}(O_l - Y_l)^2)$ is the error for training sample N, O_l and Y_l are, respectively, the predicted and desired outputs at node l. Learning algorithm is the adaptive procedure through which the network modifies the weights repeatedly to approach the goal point with the lowest error [36].

Fig. 6 shows the ANN based model used to perform estimation. The output of ANN is the predicted pre-intervention WFT risk level ($PRE\_\overline{WFT}(t+1)$). The final output of the model, the post-intervention WFT risk level ($POST\_\overline{WFT}(t+1)$) is gained by multiplying the intervention coefficient $\gamma(t)$ and ($PRE\_\overline{WFT}(t+1)$).

Following the recommendations of Negnevitsky [38], the topology of ANN comprises one hidden layer. Aiming at avoiding over-training (more neurons) and under-fitting (less neurons), the number of hidden neurons is $M = 2P + 1$ following Kolmogorov's theorem [39], where P is the number

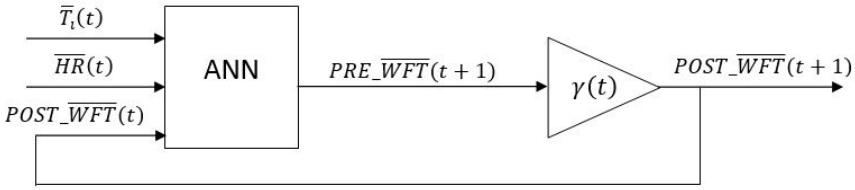

Figure 6: Architecture of the ANN-based model (WANN)

of input variables. Because data is normalized between 0 and 1, the logistic sigmoid activation functions was chosen for the output (Eq. (7)).

$$f_1(\sum_{j=1}^{P} w_{k,j}x_j + b_1^k) = \frac{1}{1 + e^{-(\sum_{j=1}^{P} w_{k,j}x_j + b_1^k)}} \tag{7}$$

Regarding the hidden layer, and using the error and trial procedure, the logistic sigmoid provided better performance than linear, hyperbolic tangent sigmoid, rectified linear unit (ReLU) and leaky ReLU activation functions [40]. The weights were uniformly distributed following Glorot's initialization algorithm [41] to break symmetry when back propagating, and to avoid the problems of exploding and vanishing gradients. The gradient descent algorithm was utilized with an adaptive learning rate (Eq. (8)). We started by a relatively large learning rate to proceed rapidly toward the good zone, which was then progressively reduced until a small rate was achieved at the end for more precision. The optimized parameters of ANN were obtained when the global error was smaller than 10^{-3}.

$$\eta(iter) = \frac{\eta_0}{\sqrt{iter}} \tag{8}$$

where $iter$ is the current learning epoch, η_0 is the initial rate (0.3), and $\eta(iter)$ is the learning rate at epoch $iter$.

2.5. Adaptive Neuro-Fuzzy Inference System

ANFIS was introduced by Jang [19] for system identification, estimation and contol, to overcome the drawbacks of ANNs and FL [42]. ANFIS is used to model complex input-output relationships because it incorporates the knowledge representation of FL and learning ability of ANNs. The most important advantage of ANFIS is that when the training process is finalized, knowledge is explicitly constituted by the fuzzy rules (gray-box comportment). ANFIS uses a Takagi-Sugeno

(or Sugeno) FIS [43] to estimate the output. The output MFs of a Sugeno FIS could be linear (first-order polynomial) or constant (zero-order polynomial). The fuzzy reasoning mechanism of a 2 input (X_1 *and* X_2) Sugeno model can be expressed as follows:

$$Rule\ 1 : If\ X_1\ is\ A_1\ and\ X_2\ is\ B_1,\ then\ y_1 = k_{01} + k_{11}X_1 + k_{21}X_2$$
$$Rule\ 2 : If\ X_1\ is\ A_2\ and\ X_2\ is\ B_2,\ then\ y_2 = k_{02} + k_{12}X_1 + k_{22}X_2$$

where $A_1, A_2, B_1\ and\ B_2$ are the fuzzy sets of X_1 and X_2, y_1 and y_2 are the linear output functions. The coefficients $\{(k_{01}, k_{11}, k_{21}), (k_{02}, k_{12}, k_{22})\}$ are the conclusion parameters of rules 1 and 2 respectively. Fig. 7 shows the architecture of ANFIS corresponding to the implementation of the above rules.

ANFIS consists of five layers in which layers 1 and 4 (squares) are adaptive (their parameters are tuneable) whereas the others are fixed (circles). The concept of ANFIS is described below.

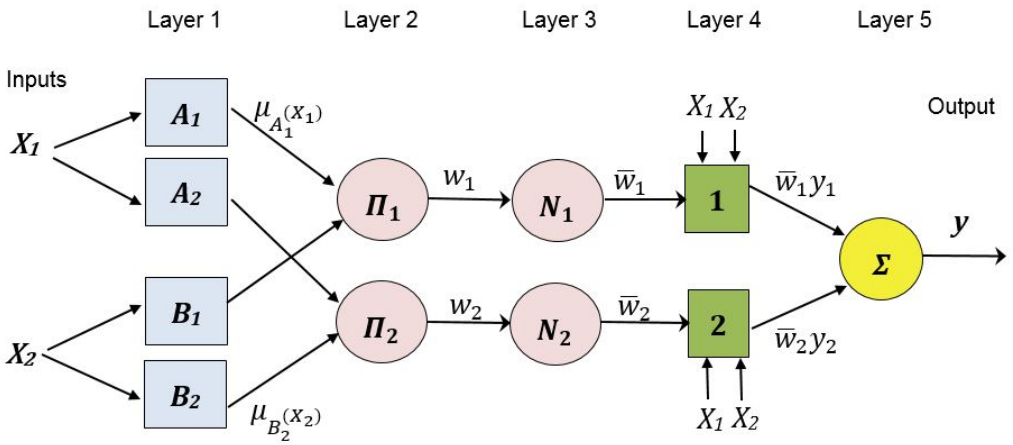

Figure 7: ANFIS structure

Layer 1: Known as the fuzzification layer where the crisp inputs are transformed into fuzzy sets. The outputs of this layer are nothing but the MFs.

$$O_{1,j} = \mu_{A_j}(X_1)\ for\ j = 1, 2 \tag{9}$$
$$O_{1,j} = \mu_{B_j}(X_2)\ for\ j = 1, 2 \tag{10}$$

where $A_j(X_1)$ and $B_j(X_2)$ are the linguistic label associated with the nodes, μ_{A_j} and μ_{B_j} are the MFs. Parameters in this layer are called the nonlinear parameters of the model, or the premise

parameters.

Layer 2: A fixed layer referred to as the rule layer. The output of each node is the firing strength of the rule described as the product ($\prod_i$) of all incoming signals.

$$O_{2,i} = w_i = \mu_{A_j}(X_1) \times \mu_{B_j}(X_2),\ i = 1, 2 \tag{11}$$

Layer 3: The firing strength of every rule i is calculated to the sum of firing strengths of all rules. Consequently, this layer is known as the normalization layer (N_i).

$$\begin{aligned} O_{3,i} = \bar{w_i} &= \frac{w_i}{\sum_i w_i} \\ &= \frac{w_i}{w_1 + w_2},\ i = 1, 2 \end{aligned} \tag{12}$$

Layer 4: This layer is known as the defuzzification layer whose nodes are adaptive in nature. The processing in this layer can be interpreted as the contribution of every rule to the overall output. The node function of the i^{th} node is:

$$O_{4,i} = \bar{w_i} y_i = \bar{w_i}(k_{0i} + k_{1i} X_1 + k_{2i} X_2),\ i = 1, 2 \tag{13}$$

where $\bar{w_i}$ is the output of layer 3, X_1 and X_2 are the inputs, and $\{k_{0i}, k_{1i}, k_{2i}\}$ are the linear (consequent) parameters.

Layer 5: This is the final layer which consists of one node only. This node calculates the overall output by summing up ($\sum$) all the incoming signals.

$$O_{5,1} = y = \sum_i \bar{w_i} y_i \tag{14}$$

$$= \bar{w_1} y_1 + \bar{w_2} y_2 \tag{15}$$

ANFIS employs a hybrid learning algorithm [19, 44] to tune its antecedent and consequent parameters.

In this study, the risk level of WFT was also evaluated by examining an ANFIS-based model (Fig. 8).

Initial partitioning of the input space was performed using the grid method. This approach is as follows: based on a predefined number of MF, the data is partitioned into fuzzy rectangular subspaces using axis-paralleled partitions. The grid method is recommended when the number of inputs is small (less than 6). It is due to the fact that the number of rules increase exponentially as the number of inputs increases, which requires a large computer memory to perform the learning.

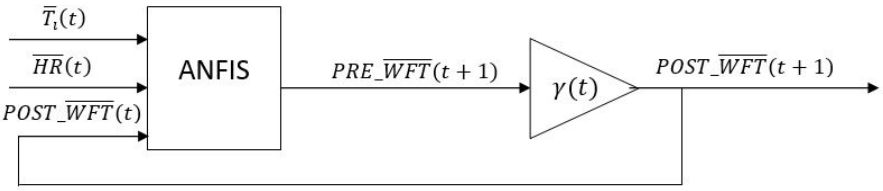

Figure 8: Architecture of the ANFIS-based model (WANFIS)

Regarding ANFIS, the Gaussian MF (Eq. (16))

$$\mu_A(x, c, \sigma) = e^{-\frac{(x-c)^2}{2\sigma^2}} \tag{16}$$

with c and σ being respectively the center and the width of the fuzzy set A, was found superior to all other types and it was consequently chosen to train the model. Based on the hybrid learning algorithm, ANFIS was trained until the training error was smaller than 10^{-3}.

2.6. Evaluation of Models Performance

The goodness-of-fit for the two models was evaluated through three statistical indicators: the coefficient of determination (R^2), root mean square error ($RMSE$) and mean absolute error (MAE). They indicate the accuracy of prediction by calculating the difference between measured and predicted values. They are defined as follows [45]:

$$R^2 = 1 - \frac{\sum_{n=1}^{N}(y_n - \hat{y}_n)^2}{\sum_{n=1}^{N}(y_n - \bar{y}_n)^2} \tag{17}$$

$$RMSE = \sqrt{\frac{1}{N}\sum_{n=1}^{N}(\hat{y}_n - y_n)^2} \tag{18}$$

$$MAE = \frac{1}{N}\sum_{n=1}^{N}|\hat{y}_n - y_n| \tag{19}$$

where $\hat{y}_n$ and y_n are respective predicted and measured WFT levels for the n^{th} data entry, and $\bar{y}_n$ is the average of y_n.

3. Results

In order to prevent the problems caused by the varying scales which often lead to under-fitting (the model could not generalize the relationship between a set of inputs and a set of outputs during

the training process), data were normalized between 0 and 1 using the maximum standardization method [46], to equalize the contribution of inputs to the prediction of the output. The training data is composed of 510 observations corresponding to the interpolated values and the testing data is constituted of 87 samples representing the real measured values.

3.1. Evaluation of WANN

The first task is to validate the neural network as it is considered the crux of the WANN model. The robustness of ANN can be regarded in Table 2 by means of high determination coefficients during training $R^2 = 0.98$ and testing $R^2 = 0.96$ phases.

Table 2: Goodness-of-fit indicators of ANN and WANN

Model	**ANN**		**WANN**	
Target	$PRE\_\overline{WFT}(t+1)$		**Actual** $POST\_\overline{WFT}(t+1)$	
			Predicted	
	Training	**Testing**	$PRE\_\overline{WFT}(t+1)$	$POST\_\overline{WFT}(t+1)$
$\mathbf{R^2}$	0.98	0.96	0.96	0.96
RMSE	0.10	0.13	0.13	0.12
MAE	0.08	0.10	0.10	0.10

In consideration of the testing phase, we can interpret that ANN explained 96% of variation between real and estimated values. In terms of RMSE and MAE, ANN illustrated a high prediction accuracy with RMSE=0.1 (3.3%) and MAE=0.08 (2.7%) for the training data, and RMSE=0.13 (4.3%) and MAE=0.1 (3.3%) when calculated for testing data.

Fig. 9 shows the correlation between predicted and actual WFT level for testing dataset. The model is very accurate showing a strong correlation between the model's predictions and its actual results. We can therefore rely on ANN to estimate WFT after intervention ($POST\_\overline{WFT}(t+1)$). The input variable human intervention γ(t) is utilized as a weighting coefficient to $PRE\_\overline{WFT}(t+1)$. The component "WANN" of Table 2 aims to demonstrate the influence of intervention of the prediction procedure. In that regard, we compute the indicators between actual thrips after intervention (Actual $POST\_\overline{WFT}(t+1)$) and that predicted before (Predicted $PRE\_\overline{WFT}(t+1)$) and after intervention (Predicted $POST\_\overline{WFT}(t+1)$). We observe that intervention provokes a slight enhancement of results (in terms of RMSE). However, they are almost identical and the influence of intervention is

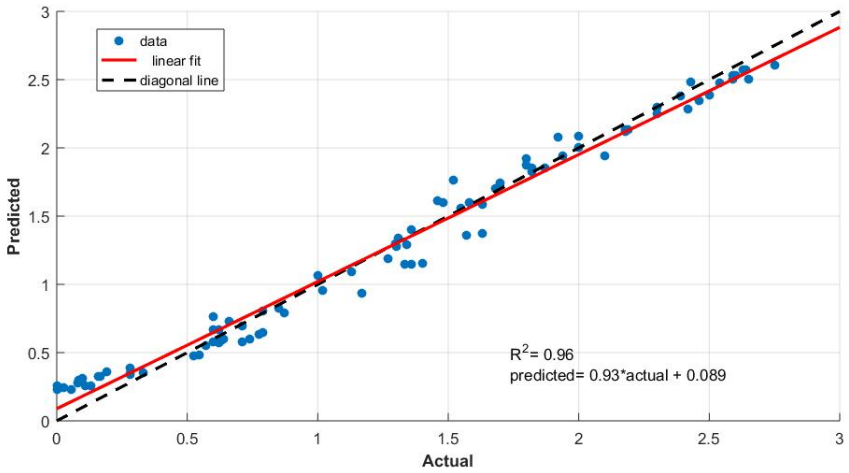

Figure 9: Scatter plot of ANN of actual versus predicted $PRE\_\overline{WFT}(t+1)$ for the testing phase

negligible because the information is included in the input of network.

3.2. Evaluation of WANFIS

Table 3 tabulates the measures of accuracy associated with ANFIS showing a high R^2 (Training: 0.99, Testing: 0.98). In terms of RMSE and MAE, ANFIS also revealed smaller error values indicating a vigorous performance. Such results justify the selection of $POST\_\overline{WFT}(t)$ in the input vector. Fig. 10 shows the correlation between predicted and actual WFT level for testing data-sets. It's trivially noticed that ANFIS is very accurate showing a strong correlation between the model's predictions and its real values.

Table 3: Goodness-of-fit indicators of ANFIS and WANFIS

Model	**ANFIS**		**WANFIS**	
Target	$PRE\_\overline{WFT}(t+1)$		**Actual** $POST\_\overline{WFT}(t+1)$	
			Predicted	
	Training	**Testing**	$PRE\_\overline{WFT}(t+1)$	$POST\_\overline{WFT}(t+1)$
$\mathbf{R^2}$	0.99	0.98	0.98	0.98
RMSE	0.06	0.11	0.11	0.11
MAE	0.05	0.08	0.08	0.08

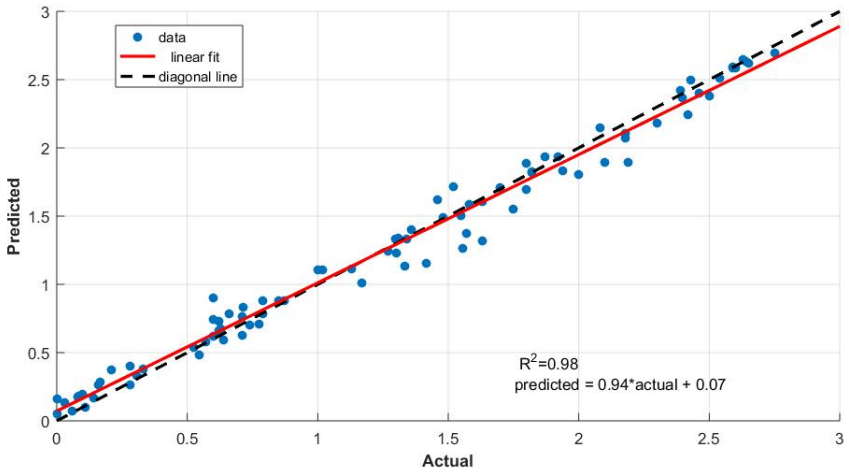

Figure 10: Scatter plot of ANFIS of actual versus predicted $PRE\_\overline{WFT}(t+1)$ for the testing phase

We therefore rely on ANFIS to estimate WFT after intervention ($POST\_\overline{WFT}(t+1)$). The variable human intervention γ(t) is utilized as a weighting coefficient to $PRE\_\overline{WFT}(t+1)$. Table 3 displays the effect of intervention on the prediction procedure no significant change is perceived. This indicates that we can neglect human intervention in its current form. It is trivial that the results with or without intervention are identical.

3.3. WANN vs WANFIS

Based on prediction results in sections 3.1 and 3.2, we compared WANN and WANFIS. Fig. 11 displays the plot of actual (full line, black-*) and estimated daily WFT risk level of WANN (dotted line, green-◇) and WANFIS (dashed line, red-o).

The plot indicates high prediction accuracy when comparing the three curves. Even though it is difficult to reveal which model is better through visualization, or by making a one-to-one comparison for the estimated values, we notice that the curve corresponding to WANFIS overlaps more perfectly with real-data curve, disclosing consistency with the results of Tables 2 and 3.

Fig. 12 presents the percentage of residuals (PE) between real and predicted values for each model (Eq. (20)).

$$PE(\%) = (real - predicted) \times 100 \tag{20}$$

The residues are small, varying between ±10% (acceptable range), upholding the high forecasting quality of both models. Results demonstrated that both are competitive. It is obvious that the

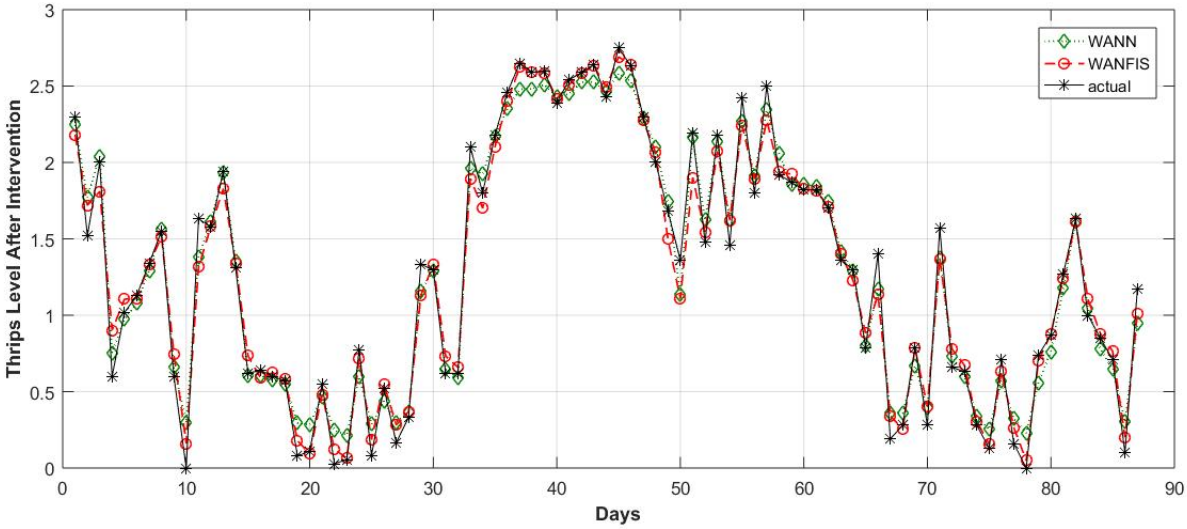

Figure 11: Actual and predicted WFT risk level after intervention

residues of WANFIS are globally smaller than those of WANN. WANFIS was found superior to WANN in terms of all statistical indicators making it considerably more reliable.

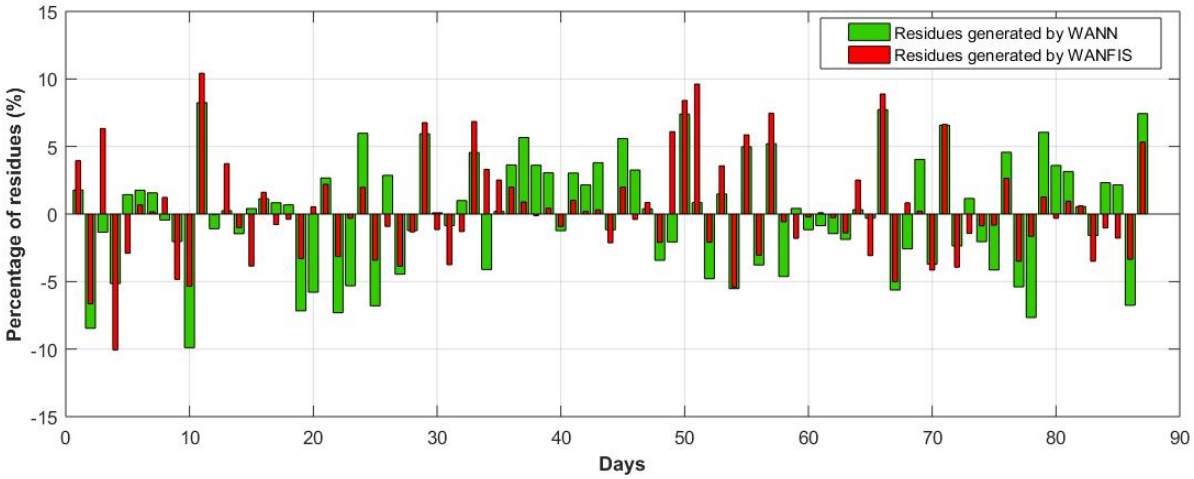

Figure 12: Daily residuals of WANN and WANFIS

The predictions generated by WANN and WANTS didn't show any statistically significant difference (Mann-Whitney U-test [47], Z=0.052, p=0.95). In other words, the medians of the two estimated populations were found equal. Besides, although the residues are small, the average percentage error

(APE) was evaluated to know if the models have the tendency to overestimate or underestimate (Eq. (21)).

$$APE(\%) = \frac{PE}{\text{total number of observations in the test phase}} = \frac{PE}{87} \tag{21}$$

Table 4 tabulates the obtained results. The negative $APE = -0.2\%$ indicates that on average, the WANN model had a tendency to overestimate. On the contrary, we observed that WANFIS possessed an underestimation tendency $APE = -0.4\%$.

Table 4: Average percentage error for WANN and WANFIS

Model	WANN	WANFIS
$APE(\%)$	-0.2%	0.4%

Based on what was interpreted above, it would more efficient to consider WANFIS because knowledge is extracted through the IF-THEN rules constructed by the system. This implies that the farmer can interpret the risk level, analyze the results, review decision making principles and conduct suitable strategies.

4. Discussion

These results were obtained upon data collected from in an experimental greenhouse, during a production period. The strengths of the models are that they are friendly-applicable by end-users, they rely on a small number of variables, and they help optimize the production and its cost (yield/pesticides). Also, they depend on real-time data, so they are self-adaptive to meteorological perturbations and seasonal variations. On the other hand, they possess some disadvantages. Like other learning models, a training data-set is required to optimize the model parameters. Collecting this data is not always possible by farmers unless some engineers are hired to do so. The achievement of study's objectives (potential of decreasing the use of pesticides and yield loss) is the most useful part for the end-user.

Moreover, the results found in this research are related to a project about designing a decision support system (DSS) for IPM in roses greenhouses. Based on the theoretical concepts used in this study, a supervision interface is being created. Hence, based on the displayed prediction, the end-user will take appropriate decisions. Since the system provides daily information, spraying pesticides could be replaced by other IPM strategies (biological, cultural, etc...), and we therefore expect a reduced pulverization of chemicals. Concerning human intervention, we saw that its effect was too small for

both models WANN and WANFIS. This is attributed to the fact that intervention information is included in each sample of the training (interpolated) and testing (real) data because we are dealing with dynamic models. An alternative could be to reset the system to certain thresholds at the end of each intervention stage. Such decision is authorized when the greenhouses is in rest mode, i.e, no interest for evaluating the risk at a certain period. Those results express the importance and ability of applying ANN and ANFIS for pest risk assessment. Knowing that some diseases such as Mildew are caused due to WFT, then early detection could avoid the contamination.

5. Conclusion

The research documented in this paper corresponds to the employment of ANNs and ANFIS models in agriculture, precisely for integrated pest management. The objective of this study is to predict the next day's WFT risk level in roses greenhouse depending on today's internal temperature and humidity, human intervention, and WFT risk level. Human intervention was found useless in its current modeling form and should be properly considered. Drawing comparison between models WANN and WANFIS demonstrated promising results for both ($R^2 = 0.96$ and $R^2 = 0.98$ respectively) with higher accuracy for WANFIS. Being ANFIS-based, WANFIS is recommended because the complexities ruling the system's behaviors are explicable through the If-Then rules generated by ANFIS. In so doing, the farmer can understand and analyze the relations between the inputs and the output, and accordingly carry out relevant programs. Two of the main contributions this study brings are the development of a risk assessment model that relies on a small number of variables (low cost, less time, more efficiency), and that provides a daily, rather than weekly, risk assessment.

6. Acknowledgments

The authors would like to thank the editor and the reviewers for their helpful comments and suggestions that led to an improved paper. We also thank Mrs. Ange Lhoste-Drouineau, project manager and engineer at the SCRADH, for supporting us with the data.

References

[1] Kirk WD. The pest and vector from the west: frankliniella occidentalis. In: Thrips and Tospoviruses: Proceedings of the 7th International Symposium on Thysanoptera. vol.2; 2002. p. 32-34.

[2] Kirk WD, Terry I. The spread of the western flower thrips frankliniella occidentalis (pergande). Agr Forest Entomol 2003;5:301-310. https://doi.org/10.1046/j.1461-9563.2003.00192.x.

[3] Morse JG, Hoddle MS. Invasion biology of thrips. Annu Rev Entomol. 2006;51:67-89.

[4] Cloyd RA. Effects of predators on the below ground life stages (prepupae and pupae) of the western flower thrips, frankliniella occidentalis (thripidae: thysanoptera): a review. Adv Entomol. 2019;7:71-80. https://doi.org/10.4236/ae.2019.74006.

[5] Mouden S, Sarmiento K, Klinkhamer P, Leiss K. Integrated pest management in western flower thrips: past, present and future. Pest Manag Sci. 2017;73(5):813-822. https://doi.org/10.1002/ps.4531.

[6] Barzman M, Barberi P, Birch ANE, Boonekamp P, Graf B. Eight principles of integrated pest management. Agron Sustain Dev. 2015;35:1199-1215.

[7] Cloyd RA. Western flower thrips (frankliniella occidentalis) management on ornamental crops grown in greenhouses: have we reached an impasse? Pest Tech. 2009;3:1-9.

[8] Hollingsworth RG, Sewake KT, Armstrong JW. Scouting methods for detection of thrips (thysanoptera: thripidae) on dendrobium orchids in hawaii. Environ Entomol. 2002;31(3):523-532.

[9] Kaas JP. Scouting for thrips - the development of a time saving sampling program for echinothrips. Proc Exper Appl Entomol. 2001;12.

[10] Pizzol J, Hervouet DNP, Desneux ABN, Mailleret L. Comparison of two methods of monitoring thrips populations in a greenhouse rose crop. J Pest Sci. 2010;83:191-196. https://doi.org/10.1007/s10340-010-0286-5.

[11] Ogada P, Moualeu D, Poehling H. Predictive models for tomato spotted wilt virus spread dynamics, considering frankliniella occidentalis specific life processes as influenced by the virus. PLoS One. 2016;11(5). https://doi.org/10.1371/journal.pone.0154533.

[12] Nothnagl M, Kosiba A, Alsanius BW, Anderson P, Larsen RU. Modelling population dynamics of frankliniella occidentalis pergande (thysanoptera: thripidae) on greenhouse grown chrysanthemum. Eur J Hortic Sci. 2008;73:12-19.

[13] Wang K, Shipp JL. Simulation model for population dynamics of frankliniella occidentalis (thysanoptera: thripidae) on greenhouse cucumber. Popul Ecol. 2001;30:1073-1081.

[14] Li WD, Zhang PJ, Zhang JM, Zhang ZJ, Huang F, Bei YW, et al. An evaluation of frankliniella occidentalis (thysanoptera: thripidae) and frankliniella intonsa (thysanoptera: thripidae) performance on different plant leaves based on life history characteristics. J Insect Sci. 2015. https://doi.org/10.1093/jisesa/ieu167.

[15] Tonnang HEZ, Hervé BDB, Biber-Freudenberge L, Salifu D, Subramanian S, Ngowi VB, et al. Advances in crop insect modelling methods—towards a whole system approach. Ecol Model. 2017;354:88-109. https://doi.org/10.1016/j.ecolmodel.2017.03.015.

[16] Wang X, Tao Y, Song X. Mathematical model for the control of a pest population with impulsive perturbations on diseased pest. Appl Math Model. 2009;33:3099-3106. https://doi.org/10.1016/j.apm.2008.10.023.

[17] Dogan I. An overview of soft computing. Procedia Comput Sci. 2016;102:34-38. https://doi.org/10.1016/j.procs.2016.09.366.

[18] McCulloch W, Pitts W. A logical calculus of the ideas immanent in nervous activity. Bull Math Biophys. 1943:115-133. https://doi.org/10.1007/BF02478259.

[19] Jang JSR. ANFIS: adaptive-network-based fuzzy inference system. IEEE T Syst Man Cy. 1993;23(3):665-685.

[20] Patil J, Mytri VD. A prediction model for population dynamics of cotton pest (thrips tabaci linde) using multilayer-perceptron neural network. Int J Comput Appl. 2013;67(4).

[21] Yan Y, Feng CC, Wan MPH, Chang KTT. Multiple regression and artificial neural network for the prediction of crop pest risks. In: Diaz P, BenSaoud N, Dugdale J, Hanachi C, editors. Information Systems for Crisis Response and Management in Mediterranean Countries. Springer; 2015. p. 73-84.

[22] Corrales D, Pena A, Leon C, Figueroa A, Corrales JC. Early warning system for coffee rust disease based on error correcting output codes: a proposal. Ingenieria y Universidad. 2014;13.

[23] Klem K, Vanova M, Hajslova J, Lancova K. A neural network model for prediction of deoxynivalenol content in wheat grain based on weather data and preceding crop. Plant Soil Environ. 2007;53:421-429.

[24] Peacock L, Worner S, Pitt J. The application of artificial neural networks in plant protection. EPPO Bulletin. 2007;37(2):277-282. https://doi.org/10.1111/j.1365-2338.2007.01123.x.

[25] Golhani K, Balasundram SK, Vadamalai G, Pradhan B. A review of neural networks in plant disease detection using hyperspectral data. Inf Process Agric. 2018;5(3):354-371. https://doi.org/10.1016/j.inpa.2018.05.002.

[26] Durgabai R, Bhargavi P, Jyothi S. Pest management using machine learning algorithms: a review. IJCSE. 2018;8(1):13-22.

[27] Kim YH, Yoo SJ, Gu YH, Lim JH, Han D, Baik SW. Crop pests prediction method using regression and machine learning technology: survey. IERI Procedia. 2014;6:52-56.

[28] Sabrol H, Kumar S. Plant leaf disease detection using adaptive neuro-fuzzy classification. In: Arai K, Kapoor S, editors. Advances in Computer Vision. CVC 2019. Advances in Intelligent Systems and Computing,. vol. 943. Springer, Cham; 2020. p. 434-443.

[29] Mayannavar SM, Sangani SP, Gollagi SG, Huddar MG, Pawar MR. Adaptive neuro-fuzzy inference system for recognition of cotton leaf diseases. IJSDR. 2016;1(8).

[30] Rahmon IA, Adebola A, Eze MO. A neuro-fuzzy system for diagnosis of soya-beans diseases. RJMCS. 2018;2(13).

[31] Tay A, Lafont F, Balmat JF, Pessel N, Lhoste-Drouineau A. Fuzzy approach to pest risk assessment in a greenhouse. In: 22nd International conference on smart decision-making systems for precision agriculture, Madrid; 2020. p. 1943-1949.

[32] Olatinwo R, Hoogenboom G. Weather-based pest forecasting for efficient crop protection. In: Abrol DB, editor. Integrated pest management: current concepts and ecological perspective. Academic Press, Elsevier; 2014. p. 59-78.

[33] Fatnassi H, Pizzol J, Senoussi R, Biondi A, Desneux N, Poncet C, et al. Within crop air temperature and humidity outcomes on spatio-temporal distribution of the key rose pest frankliniella occidentalis. PLoS One. 2015;10(5). E0126655. https://doi.org/10.1371/journal.pone.0126655.

[34] Steiner M, Spohr L, Goodwin S. Relative humidity controls pupation success and dropping behaviour of western flower thrips, frankliniella occidentalis (pergande) (thysanoptera: thripidae). Aust J Entomol. 2011;50:179-186. https://doi.org/10.1111/j.1440-6055.2010.00798.x.

[35] Muthumalai RK. Note on newton interpolation formula. Int J Math Anal. 2012;6(50):2459-2465.

[36] Rezaeianzadeh M, Tabari H, Yazdi AA, Isik S, Kalin L. Flood flow forecasting using ANN, ANFIS and regression models. Neural Comput Appl. 2014;25:25-37. https://doi.org/10.1007/s00521-013-1443-6.

[37] Hagan MT, Menhaj M. Training feedforward networks with the marquardt algorithm. IEEE T Neural Networ. 1994;5(6):989-993. https://doi.org/10.1109/72.329697.

[38] Negnevitsky M. Artificial neural networks. In: Negnevitsky M, editor. Artificial intelligence : a guide to intelligent systems (second edition). Addison-Wesley; 2005. p. 165-212.

[39] Kolmogorov A. On the representation of continuous functions of several variables by superposition of continuous functions of one variable and addition. Doklady Akademii Nauk USSR. 1957;114:679-681.

[40] Wang Y, Li Y, Song Y, Rong X. The influence of the activation function in a convolution neural network model of facial expression recognition. Appl Sci. 2020;10(5):1897. https://doi.org/10.3390/app10051897.

[41] Glorot X, Bengio Y. Understanding the difficulty of training deep feedforward neural networks. J Mach Learn Res. 2010;9:249-256.

[42] Sakunthala S, Kiranmayi R, Mandadi PN. A review on artificial intelligence techniques in electrical drives: neural networks, fuzzy logic, and genetic algorithm. In: 2017 International conference on smart technologies for smart nation; 2017. p. 11-16. https://doi.org/10.1109/SmartTechCon.2017.8358335.

[43] Takagi T, Sugeno M. Fuzzy identification of systems and its applications to modeling and control. IEEE T Syst Man Cy. 1985;15:116-132.

[44] Jang JSR, Sun CT. Neuro-fuzzy modeling and control. P IEEE. 1995;83(3):378-406.

[45] Olyaie E, Banejad H, Chau KW, Melesse AM. A comparison of various artificial intelligence approaches performance for estimating suspended sediment load of river systems: a case study in united states. Environ Monit Assess. 2015. https://doi.org/10.1007/s10661-015-4381-1.

[46] Anysz H, Zbiciak A, Ibadov N. The influence of input data standardization method on prediction accuracy of artificial neural networks. Procedia Eng. 2016;153:66-70. https://doi.org/10.1016/j.proeng.2016.08.081.

[47] Nachar N. The Mann-Whitney U: a test for assessing whether two independent samples come from the same distribution. Tutor Quant Methods Psychol. 2008. https://doi.org/10.20982/tqmp.04.1.p013.